

AN EXPERIMENTAL INVESTIGATION OF THE EFFECT OF ASPECT RATIO ON THE AIRFOIL PERFORMANCE

Rehan Uddin^{1,*}, Md. Assad-Uz-Zaman², Rubiat Mustak³ and Mohammad Mashud⁴

¹⁻⁴Department of Mechanical Engineering, Khulna University of Engineering & Technology, Khulna-9203,
BANGLADESH

^{1,*}Rehan.uddin.002@gmail.com, ²assad_kuet08@yahoo.com, ³rubiatpantho@gmail.com, ⁴mdmashud@yahoo.com

Abstract- In this experiment, the effect of aspect ratio on the airfoil performance are investigated. The objective of this experiment is to find the effect of this ratio on the airfoil performance for same wingspan but different chord. Three samples of different aspect ratios such as $AR=1.83$, $AR=2.2$ and $AR=2.75$ of asymmetrical airfoils type NACA 2412, were tested in this experiment, with different attack angles from 0 to 20 degrees, at constant wind speed of about 25 m/s. . The test conducted in subsonic wind tunnel of $1m \times 1m$ rectangular test section, its maximum wind speed is about 43 m/s. The results of this experiment clarify that the Aspect Ratio (AR) has an important effect on the aerodynamic performance of the airfoils. Finally, the results show that the optimal performance was achieved at $AR=1.83$ with angles of attack ranging from 6 degree to 12 degree with wind speed of 25m/s.

Keywords: Air flow, Airfoil Performance, Lift Coefficient, Drag Coefficient.

1. INTRODUCTION

The lifting surface of an immersed body may be defined as a tool which develops a useful reaction force during its motion relative to the fluid. The surfaces of wings and tails of aero planes, propellers and blades of turbo machinery are some of the examples of the lifting surfaces. The optimum design of lifting surface yields the production of the maximum possible lift force and the production of the minimum possible drag force in directions perpendicular to the direction of motion. Aerodynamic performance of wings in low Reynolds number regime is typically low because of unexpected flow separation. An interference drag between wing and body also plays an important effect. Some studies dealing with numeric solution of fluid flow around wings exists, for examples [1-3]. In these studies the Allen method is used which is an extension to the potential flow theory. In the following investigations [4, 5] Boundary layer and potential flow theories are considered together. Obayashi and Takanashi used the genetic optimization method for the optimization of pressure distribution over wings [6]. Using numerical methods Raughunathan and Mitchell determined the effect of heat transfer in transonic flow about the NACA 0012 airfoil [7]. Kerho and Bragg [8] investigated the effect of surface roughness on the attack side of an airfoil on the formation of a boundary layer. Yilmaz [9, 10] experimentally investigated the performance of NACA 0012 profile with three different aspect ratios at different subsonic flow speeds in the wind tunnel. Kopac and Gultop [11] experimentally

investigated the performance of NACA 0012 profile with three different aspect ratios at same subsonic flow speeds in the wind tunnel. Caroglia and Jones [12] investigated a methodology for the experimental extraction of indicial functions for streamlined and bluff deck sections. In the present study lift and drag coefficients of three different profiles at the flow speed 25m/s are determined using experimental data. Hence, an optimum airfoil is obtained for the corresponding flow speed. The goal of this research to investigate the effect of aspect ratio on the airfoil performance.

2. AIRFOIL DESIGN & DESCRIPTION

The airfoil sections of all NACA families considered herein are obtained by combining a mean line and a thickness distribution. The necessary geometric data and some theoretical aerodynamic data for the mean lines and thickness distributions obtained from the supplementary figures by the methods described for each family of airfoils. The process for combining a mean line and a thickness distribution to obtain the desired cambered airfoil section is shown in Fig 1 below.

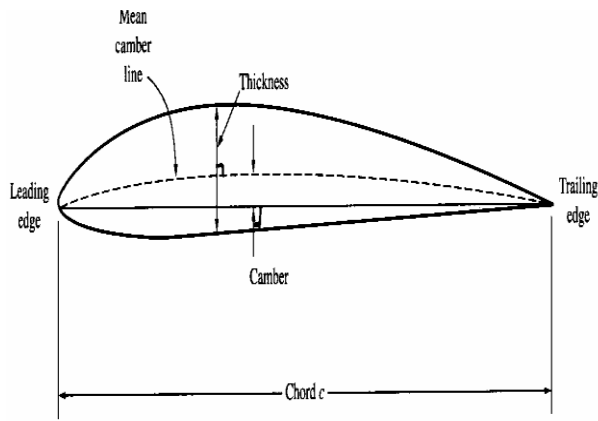


Fig.1: A typical Airfoil

The cross sectional shape obtained by the intersection of the wing with the perpendicular plane is called an airfoil. The major design feature of an airfoil is the mean cambered line, which is the locus of points halfway between the upper and lower surfaces as measured perpendicular to the mean cambered line itself. The most forward and rearward points of the mean cambered line are the leading and trailing edges respectively. The straight line connecting the leading and trailing edges is the chord line of the airfoil and the precise distance from the leading to the trailing edge measured along the chord line is simply designated the chord of the airfoil, given by the symbol C . The camber is the maximum distance between the mean camber line and the chord line, measured perpendicular to the chord line. The camber, the shape of the mean camber line and to a lesser extent, the thickness distribution of the airfoil essentially controls the lift and moment characteristics of the airfoil. For symmetrical airfoil the mean camber line coincide with chord line.

If X_u and Y_u represent respectively the abscissa and ordinate of a typical point of the upper surface of a symmetrical airfoil and y_t is the ordinate of the symmetrical thickness distribution at chord wise position X_1 , the upper surface coordinates are given by the following relations:

$$X_u = x$$

$$Y_u = y_t$$

The corresponding expressions for the lower surface co-ordinates are

$$X_l = x$$

$$Y_l = -y_t$$

2.1 AIRFOIL DESCRIPTION AF NACA 2412

For NACA 2412

Chord of airfoil, $c = 1$

For asymmetric airfoil mean chamber line coincide with chord line so for NACA 2412, there is maximum chamber in hundredths of chord

$$2 \times c / 100 = 0.02c$$

Location of maximum camber along the chord from the leading edge in tenths of chord,

$$4 \times c / 10 = 0.4c$$

Maximum thickness of the airfoil in hundredths of chord,

$$\begin{aligned} \text{Maximum wing thickness, } t &= \text{last two digit} \times \%c \\ &= 12 \times 1/100 \\ &= 0.12 \end{aligned}$$

By applying C++ Programming Language the surface profile of the airfoil was generated by using basic equation of airfoil.

The thickness and camber of such airfoils are computed as follows:

$$\pm y_t = \frac{t}{0.2} \left(0.2969\sqrt{x} - 0.1260x - 0.3516x^2 + 0.2843x^3 - 0.1015x^4 \right)$$

$$y_c = \frac{m}{p^2} (2px - x^2) \quad \text{from } x = 0 \text{ to } x = p$$

$$y_c = \frac{m}{(1-p)^2} [(1-2p) + 2px - x^2] \quad \text{from } x = p \text{ to } x = c$$

Where,

x = coordinates along the length of the airfoil, from 0 to c (which stands for chord, or length)

y = coordinates above and below the line extending along the length of the airfoil, these are either y_t for thickness coordinates or y_c for camber coordinates

t = maximum airfoil thickness in tenths of chord (i.e. a 12% thick airfoil would be 0.12)

m = maximum camber in tenths of the chord

p = position of the maximum camber along the chord in tenths of chord

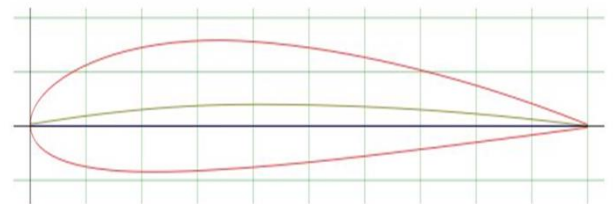


Fig.2: NACA 2412 airfoil

3. MODEL CONSTRUCTION

By applying Computer C++ Programming Language the regular surface profile of the NACA 2412 model was made. The three chord length of the model is 20 cm, 25 cm and 30 cm with same wingspan of 55 cm respectively. Thus the chord length based Reynolds number relevant at low flight speeds, which are a concern for the exploration of wing formation mechanism, is estimate to be about 105. The chord length of the model was determined to have Reynolds number of the same order. The span length of the model, relative to the chord length is one of the important design parameters. Obviously, it should be made as large as possible so that the weight of the model can be reduced. To ensure the aerodynamic characteristics of an airfoil, it is important that the trailing edge of the model have a sharp edge form. For three different aspect ratio, keeping wingspan fixed and changing chord three airfoil model was constructed shown in the figure below. The airfoil used to construct the whole structure is NACA 2412. Now models are ready for testing.



Fig.3: Constructed airfoil for AR 2.75



Fig.4: Constructed airfoil for AR 2.20



Fig.5: Constructed airfoil for AR 1.83

4. EXPERIMENTAL SETUP

Experiments were conducted in the Aerodynamics Laboratory Department of Mechanical Engineering (Khulna University of Engineering & Technology) with subsonic wind tunnel of 1 m× 1 m rectangular test section. The wind tunnel could be operated at a maximum air speed of 43 m/s and the turntable had a capacity for setting an angle of attack of 45 degree. A small sized model is appropriate to examine the aerodynamic characteristics for the experiments. If we desire to examine the aerodynamic characteristics of a large model, a large scale wind tunnel facility is necessary for testing or the inflatable wing must be drastically scaled down to match the usual wind tunnel size violating the Reynolds number analogy requirements. Furthermore, it would be difficult to support the inflatable airfoil a desirable attitude in these wind tunnel experiments. Since the vertical part of the aerodynamic force produces the lifting force necessary to suspend the load. We are mainly interested in the aerodynamic characteristics of each model. The model was placed in the testing section of the wind tunnel. Then the testing procedure is started of measuring the pressure of the constructed model at different point from leading edge to trailing edge along chord line from the pressure sensor reading. Fig 4.1 shows a photograph of the airfoil model, which is mounted horizontally in the test section of the wind tunnel.



Fig.6: Schematic diagram of the airfoil setup

5. EXPERIMENTAL PROCEDURE

For the complete testing the constructed model, subsonic wind tunnel and pressure measuring instrument were used as required apparatus. At the first step of the experimental procedure the constructed airfoil with NACA 2412 with AR 2.75 was placed inside the testing section of the wind tunnel. By placing airfoil with AR 2.75 the testing section was closed to start the measurement. For different angle of attack pressure on the upper and lower surfaces were measured. After this the airfoil along with AR 2.2 was placed in the wind tunnel and pressures on the upper and lower surfaces were measured. At last the airfoil with AR 1.83 was placed inside the wind tunnel and similar test procedures were conducted as explained earlier. The velocity of the wind tunnel was controlled by a regulator attached with the wind tunnel. The ambient pressure, temperature and humidity were recorded using barometer, thermometer, and hygrometer respectively for the evaluation of air density in the laboratory environment. The tests were carried out with free-stream velocity of 25m/s. When the measurement of data had been complete then the calculation process was started. From the measured pressure the lift coefficient and drag coefficient was calculated by using the mathematical relation. Coefficient lift to coefficient drag ratio was calculated from the lift coefficient and drag coefficient. Lift and drag coefficient can be defined as follow

$$C_L = \frac{1}{c} \int_0^c (C_{pl} - C_{pu}) dx$$

$$C_D = \frac{1}{c} \int_0^c (C_{pl} \frac{dy}{dx} - C_{pu} \frac{dy}{dx}) dx$$

Where,

C_{pl} = pressure coefficient at lower surface

C_{pu} = Pressure coefficient at upper surface

Pressure coefficient is defined as,

$$C_p = \frac{P - P_\infty}{\frac{1}{2} \rho_\infty v_\infty^2}$$

Where,

P = local pressure

P_∞ = free stream pressure

v_∞ = Free stream velocity

ρ_∞ = Free stream density

μ_∞ = Free stream viscosity

6. RESULT & DISCUSSION

Wind tunnel measurements using the constructed airfoil model for AR 2.75, AR 2.2 and AR 1.83 were done. The lift coefficient and the drag coefficient have been calculated from the experimental results. Comparison curve of pressure coefficient for different aspect ratio have been drawn. Also lift coefficient vs angle of attack, drag coefficient vs angle of attack and lift coefficient to drag coefficient ratio vs angle of attack have been plotted. The lift coefficient characteristics of the airfoil model under test are shown in Figure 6.5. The lift increases with increase in angle of attack to a maximum value and thereby decreases with further increase in angle of attack. For AR 1.83 the maximum value of the lift coefficient is 1.21 and this maximum values occur at an angle of attack of 12 degree. At the maximum angle of attack of 20 degree the lift coefficient is 0.78. The reason for a drop in lift coefficient beyond a certain angle of attack e.g. 12 degree is probably due to the flow separation, which occurs over the wing surface instead of having a streamlined laminar flow there. This condition is called stalling condition and the corresponding angle of attack is called stalling angle. The stalling angle happens to be approximately 12 degree. Other two curve for AR 2.2 and 2.75 are given in figure 4.1.15. Here from figure it is also seen that for AR 2.2 the maximum value of the lift coefficient is 1.12 and for AR 2.75 the maximum value of the lift coefficient is 1.04. So from the figure it is clearly observed that for AR 1.83 maximum value lift coefficient is obtained.

The drag coefficient of the aircraft wing model under test is shown in Figure 6.6. The drag increases slowly with increase in angle of attack to a certain value and then it increases rapidly with further increase in angle of attack. The value of the drag coefficient at the transition point i.e. at an angle of attack of 10 degree for AR 1.83, AR 2.2 and AR2.75 are respectively 0.097, 0.112 and 0.153. The value of the drag coefficient at an angle of attack of 12 degree for AR 1.83, AR 2.2 and AR2.75 are respectively 0.156, 0.196 and 0.224. The experiments have been done up to an angle of attack of 20 degree. The rapid increase in drag coefficient, which occurs at higher values of angle of attack, is probably due to the increasing region of separated flow over the wing surface, which creates a large pressure drag. The other details of the drag coefficients are given in the curve.

The lift coefficient/drag coefficient ratio is the outcome of the observations made in the two preceding sections. It is observed from the Fig. 6.7 that the lift coefficient/drag coefficient ratio for all the configurations considered increases with an angle of attack to its maximum value and thereby it decreases with further increase in angle of attack. In particular it is observed that the maximum lift coefficient/drag coefficient ratio for all the configurations considered in the study falls in the range of 2 to 10 degrees of angle of attack. The airfoil model of AR 2.75 gives a measured lift coefficient/drag coefficient ratio of 10.9 whereas the respective values of the lift coefficient/drag coefficient ratio for the AR 2.2 and AR 1.83 are 10.904, and 10.338 respectively at an angle of

attack of 2 degree. The lift coefficient/drag coefficient ratio values for the angle of attack of 10 degree are 6.27, 9.375, and 11.443 for airfoil model of AR 2.75, AR 2.2 and AR 1.83 respectively. According to the definition of Aspect Ratio we know that it is the ratio of wingspan to the chord. Mathematically,

$$A.R. = \frac{b}{c}$$

From the above relation it is inevitable that, Aspect ratio decreases with constant wingspan and increases with the chord. Chord is the distance between leading edge and trailing edge. Increasing the chord increases the curvature of the upper and lower surfaces of the airfoil. This curvature greatly influences in generating lift. An airfoil takes advantage of Bernoulli's principle. Since, the curvature i.e. increase in chord facilitates the top surface of the wing more camber than the bottom camber. The air flows faster over the top of the wing than it does underneath. This means that there is less air pressure above the wing than there is beneath the wing. The difference in air pressure above and below the wing causes lift. Hence as per the formulation, it can be thereby conclude that, for constant wingspan and increasing chord, Aspect Ratio will decrease and hence lift will increase.

Again, In contrast, a low aspect ratio wing allows the high pressure on the bottom of the wing to escape more easily, resulting in a larger vortex.

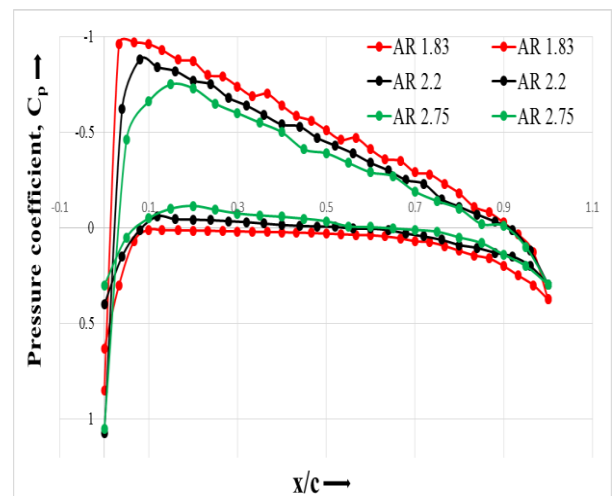


Fig.7: Comparison curve of pressure coefficient for 2 degree AOA

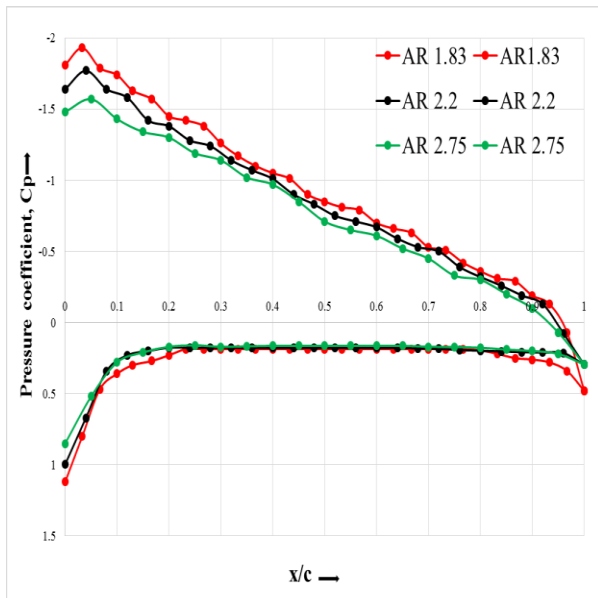


Fig.8: Comparison curve of pressure coefficient for 12 degree AOA

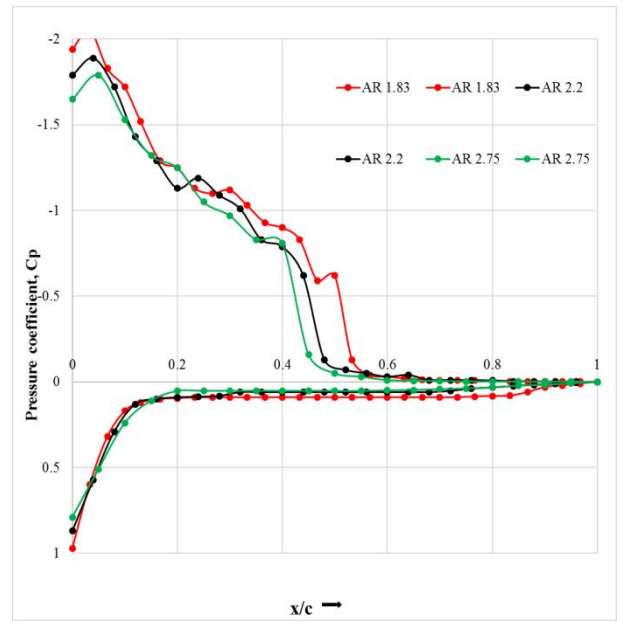


Fig.10: Comparison curve of pressure coefficient for 18 degree AOA

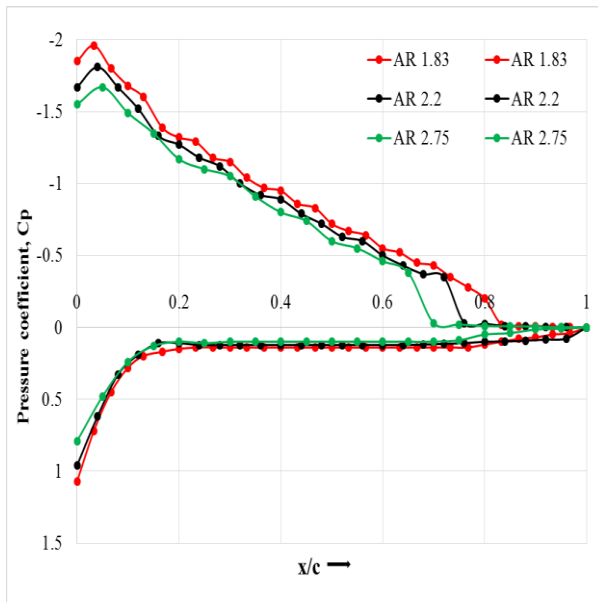


Fig.9: Comparison curve of pressure coefficient for 14 degree AOA

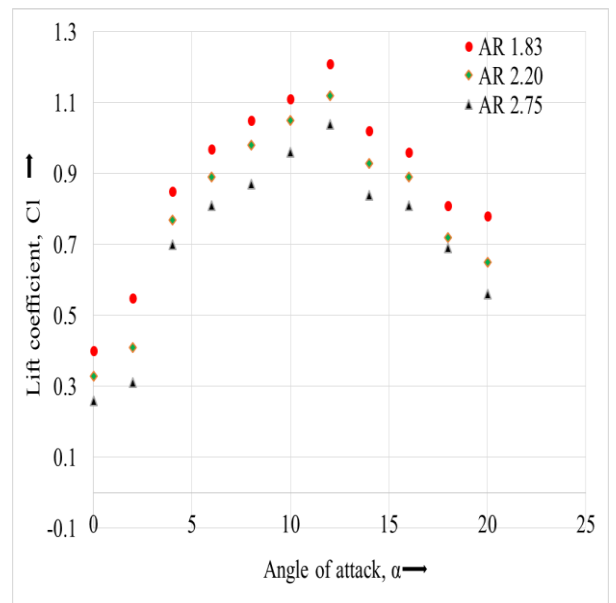


Fig.11: Lift coefficient vs angle of attack

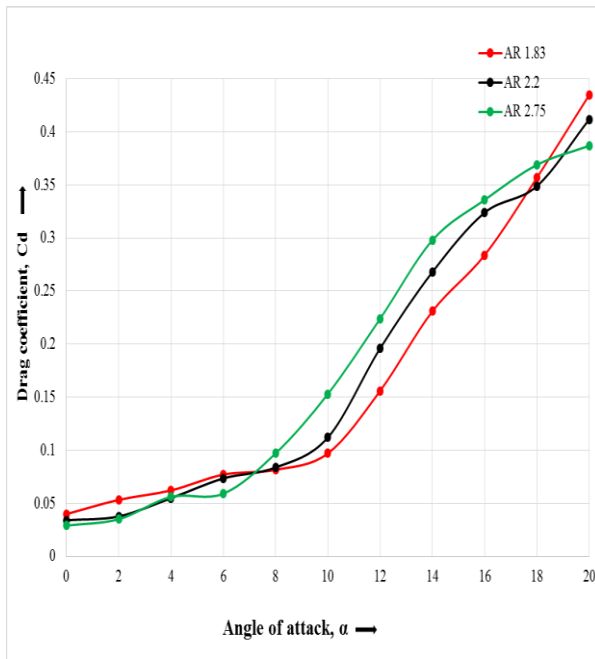


Fig.12: Drag coefficient vs angle of attack

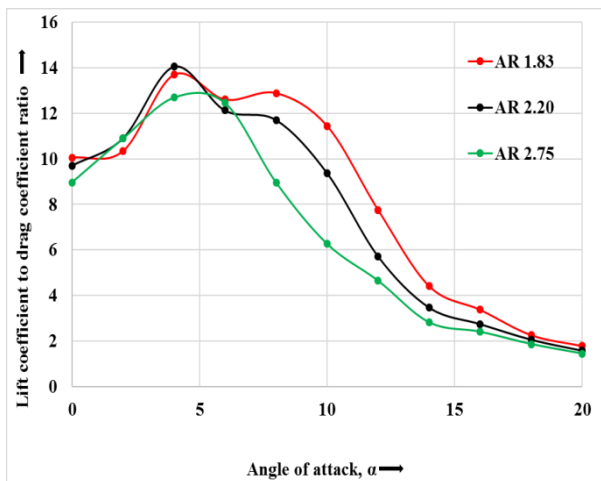


Fig.13: Lift coefficient to drag coefficient ratio vs angle of attack

7. ACKNOWLEDGEMENT

My sincere acknowledgments to Dr. Mohammad Mashud, Professor of the Department of Mechanical Engineering of Khulna University of Engineering & Technology (KUET) for his support and guidance.

8. REFERENCES

- [1] Elbay, K., 1991. Aerodynamics characteristics of axially symmetric bodies. M.Sc. Thesis stanbul Technical University, Turkey.
- [2] Telceker, N., K. Albay and V. Atli, 1991. The analytical and experimental determination of Aerodynamic characteristics of some symmetric missiles with sharp and blunt noses. Research Report, Turkish Council for Scientific and Industrial Research, Ankara, Turkey.
- [3] Atli, V., M.K. Elbay, O. Iday, H. Acar, M.

- Kazilirmak and A. Tezel, 1992. Surface flow detection and the characteristics of a MKEK 500 pounds bomb at subsonic velocities, rocket and missiles Aerodynamics. Research Report, stanbul Technical University, Turkey.
- [4] Filippone, A., 1995. Airfoil inverse design and optimization by means viscous-inviscid techniques. J. Wind Eng. Ind. Aerody., 2-3:123-136.
- [5] Sqrnsen, J.N. and A. Filippone, 1997. Viscous-inviscid interaction using navier-stokes equation. AIAA J., 35:1464-1471.
- [6] Obayashi, S. and S. Takanashi, 1996. Genetic optimization of target pressure distribution for inverse design methods. AIAA J., 30: 881-886.
- [7] Raughunathan S. and D.Mitchell, 1995. Computed effect of heat transfer in transonic flow over an airfoil. AIAA J., 33:2120-2127.
- [8] Kerho, J. and M.B Bragg, 1997. Airfoil boundary layer development and transition with large leading edge roughness. AIAA J., 35: 75-84.
- [9] Yilmaz, M. 1999. The determination of optimum geometry of various bodies in a flow field. M.Sc. Thesis. Zonguldak Karaelmas University, Turkey.
- [10] Kopac M. and M. Yilmaz, 1998. The determination of drag and lift coefficients and the geometrical optimization of various wings. Research Report, Zonguldak Karaelmas University, Turkey.
- [11] Kopac M., M. Yilmaz and T. Gultop, 2005. An investigation of the effect of aspect ratio on the airfoil performance. AJAS 2 (2): 545-549. ISSN 1546-9239.

9. NOMENCLATURE

Symbol	Meaning	Unit
L	Lift force	N
D	Drag force	N
C_l	Coefficient of lift	Dimensionless
C_d	Coefficient of drag	Dimensionless
v_∞	Free stream velocity	m/s
ρ_∞	Free stream density	kg/m ³
μ_∞	Free stream viscosity	m/s
α	Angle of attack	degree
T	Maximum thickness	m
C	Chord length	m
AOA	Angle of attack	degree